



Technical Note

Similarity and dissimilarity of electromagnetic radiation from carbonate rocks under compression, drilling and blasting

A. Rabinovitch^{a,*}, D. Bahat^b, V. Frid^b^a *The Deichmann Rock Mechanics Laboratory of the Negev, Physics Department, Ben Gurion University of the Negev, Beer Sheva, Israel*^b *The Deichmann Rock Mechanics Laboratory of the Negev, Department of Geological and Environmental Sciences, Ben Gurion University of the Negev, Beer Sheva, Israel*

Accepted 14 February 2002

1. Introduction

Numerous investigations have examined different aspects of electromagnetic radiation (EMR) emitted by fracture [1–6]. For example, it was noted that an increase of Young modulus, strength, and loading rate enhances the EMR amplitude [3,7–9]. Individual EMR pulses were carefully investigated under uniaxial and triaxial stiff compression [8–11]. An example of an EMR pulse from chalk compression is shown in Fig. 1. It is known now that a propagating crack consists of atomic bond severage, which excites atomic (or ionic) oscillations along the crack surfaces. These oscillations (Rayleigh-type waves) induce electromagnetic radiation. Hence, each crack constitutes a source of an individual EMR pulse. The EMR amplitude is a function of the crack area [12,13]; the time from the pulse origin to the maximum of its envelope, is proportional to the crack length; the frequency of the EMR pulse is related to the crack width [12,13]. An analysis of the EMR pulses emanating during uniaxial compression [14] showed that individual short pulses (of duration of 0.5–6 μ s, Table 1) are correlated with the stage of individual micro-cracks formation; multi-pulse strings are correlated with the crack coalescence stage; and lengthy pulses (of duration of 30–400 μ s, Table 1) are correlated with rock failure.

All these investigations were carried out in the laboratory. Large-scale EMR studies prior to rockbursts in mines and to earthquakes (EQ) are also registered. Thus, Khatiashvili [15] carried out an investigation of

EMR in the Tkibulli deep shaft (Georgia) prior to an EQ of a 5.4 magnitude. The registration point (at the shaft position) was located 250 km from the EQ epicenter. Prior to the EQ itself, an increase of intensity of the lower part of the spectrum (1–100 kHz) and a corresponding decrease of intensity of higher frequencies (100–1000 kHz) were observed. Nesbitt and Austin [16] registered EMR in a gold mine (2.5 km depth). Frid [17,18] observed EMR anomalies before rockbursts and gas outbursts.

It is claimed [19] that an abnormally high-EMR level occurs hours or even days before an EQ, after which EMR decreases. Rikitake [20], analyzing 60 EQ events measured in Japan, also showed that EMR is a “short-term” precursor, with an estimated mean time prior to an EQ of \sim 6 h. It was assumed [21–25] that the anomalies of EMR prior to an EQ were due to a deformation of the Earth surface, which resulted in the formation of micro-fractures and in friction of the nearby rock blocks.

Parrot et al. [26], after a detailed consideration of a large number of EMR–EQ investigations, remarked that although the existence of EMR in relation to seismic and/or volcanic activities were clear, EMR selection out of a host of artificial signals remained a significant problem. Nevertheless, investigations of EMR as a precursor to large-scale failure continue.

In this work, we present the results of our EMR investigations on carbonate rock fracture both in the large scale (blasting in an open quarry) and in the micro-scale (drilling in the lab) and show the similarities and dissimilarities of these EMR results to our previous EMR laboratory studies during regular compression tests in the laboratory.

*Corresponding author. Tel.: +972-7-646-1172; fax: +972-7-647-2904.

E-mail address: avinoam@bgumail.bgu.ac.il (A. Rabinovitch).

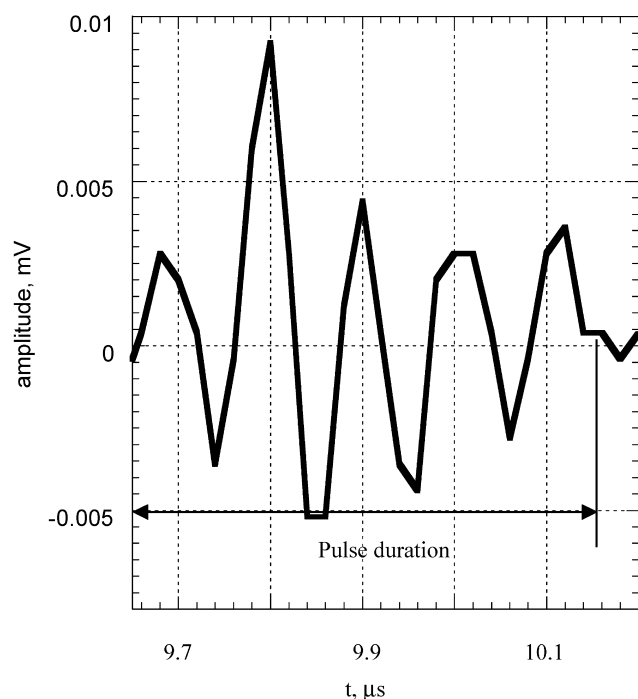


Fig. 1. An experimental EMR pulse induced by chalk compression.

2. Experimental details

2.1. Drilling

Our drilling experiments were considered in detail in Goldbaum et al. [27]. We provide here only a concise account of the experimental procedure.

2.1.1. Rocks

The samples were chalk from Ramat Hovav (20 km south to Beer Sheva, Israel [10,11]) and limestone from Solenhofen (South Germany) [28].

2.1.2. Experimental arrangement [27]

EMR measurements during drilling were carried out on cylindrically shaped samples 100 mm in length and 25 mm in diameter (Fig. 2) that were percussion drilled (impact rate of 50 Hz). Drilling was carried out at about the mid-length of the cylinder, perpendicular to the cylinder axis.

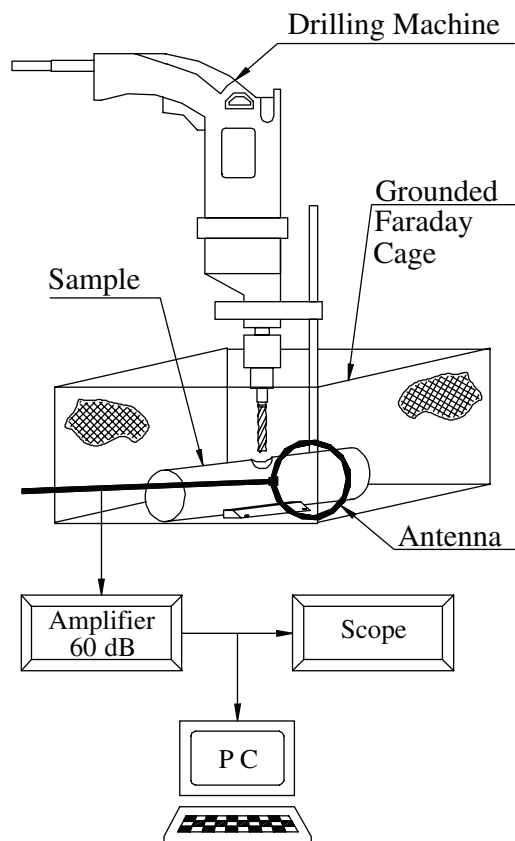


Fig. 2. Schematic diagram of experimental arrangement during drilling.

2.1.3. EMR measurement

EMR was measured in the frequency range 1 kHz–50 MHz with 1 μ V sensitivity throughout by a one-loop magnetic antenna 3 cm in diameter, which is electrically “small” and exhibits negligible response to foreign electric fields. The antenna was placed at a distance of 3 cm from the drilling hole. External electromagnetic disturbances were decreased by the two following methods: the sample together with the antenna were placed in a grounded Faraday cage, and the plane of the antenna was aligned perpendicular to the drilling direction, so that the influence of electromagnetic disturbances emitted by the motor of the drilling machine was minimized. All EMR signals were electrically amplified, digitized and collected at a triggered

Table 1
Properties of EMR pulses excited by compression, drilling and blasting

| Process | Pulse duration | | Pulse frequency | | Pulse strings' duration |
|-------------|-----------------|----------------|-----------------|---------|-------------------------|
| | Short | Lengthy | Short | Lengthy | |
| Compression | 0.5–6 μ s | 30–400 μ s | <10 MHz | >15 kHz | <30 μ s |
| Drilling | 0.3–1.5 μ s | 10–800 μ s | 10–25 MHz | >5 kHz | 2–60 μ s |
| Blasting | <3 μ s | — | 2–8 MHz | — | 0.3–0.5 s |

PC hard disk. The data were analyzed after test completion.

2.2. Blasting

2.2.1. Rock

Blastings were carried out in Turonian age limestone from an open quarry near the village Omarim, located about 25 km north-east of Beer Sheva (Israel).

2.2.2. Method

Two blasts of 5 and 1.4 t of explosion material, respectively, were performed. In each blast one slope of the quarry was exploded. The slopes heights are of about 11 m and of lengths of about 100 and 20 m, respectively.

2.2.3. EMR arrangement

A magnetic one-loop antenna (Electro-Metrics Penril Corporation) 0.5 m in diameter was used for the detection of the EMR. A low-noise micro-signal amplifier (Mitek Corporation Ltd, frequency range 10 kHz–500 MHz, gain 60 ± 0.5 dB, noise level 1.4 ± 0.1 dB throughout) and an analog-to-digital converter connected to a triggered PC completed the detection equipment. We placed our magnetic antenna in front of the blasted slope at a distance of about 100 m from it (Fig. 3).

3. Research results

3.1. Drilling

The EMR signals measured during percussion drilling could be classified into four groups [27]. The first three groups relate to: individual EMR signals (the first group

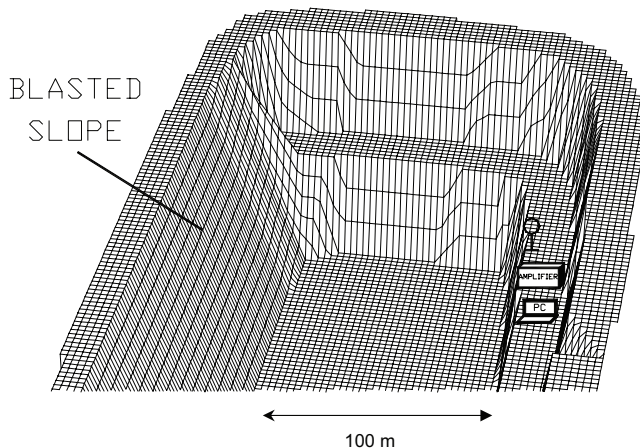


Fig. 3. Schematic diagram of experimental arrangement during blasting.

of signals having durations of 0.3–1.5 μ s, Table 1), signals arriving in short strings (string duration of 2–15 μ s—second group, Table 1) and extended signals of larger duration (up to 60 μ s—third group, Table 1). The individual EMR signals correspond to single micro-cracks (from 0.005 mm² up to about 0.05 mm² in area) while signals of the second and third groups are related to overlapping of such micro-cracks. The fourth group of EMR signals [27] possibly originates from lengthy fractures (up to several centimeters in area).

Figs. 4a and b show two examples of EMR signals of the second and third group observed during drilling of Solenhofen limestone and Ramat Hovav chalk, respectively. Note that the shapes of the EMR strings emanating from these rocks are similar to each other, the only difference lies in their durations that were of about 10 and 60 μ s, respectively. Zooming in on both signals shows that they consist of numerous individual signals of frequencies of 10–25 MHz (Table 1). Fig. 5 shows an example of a string of three individual EMR signals from chalk drilling. A comparison of Figs. 1 and 5 shows that shapes of individual

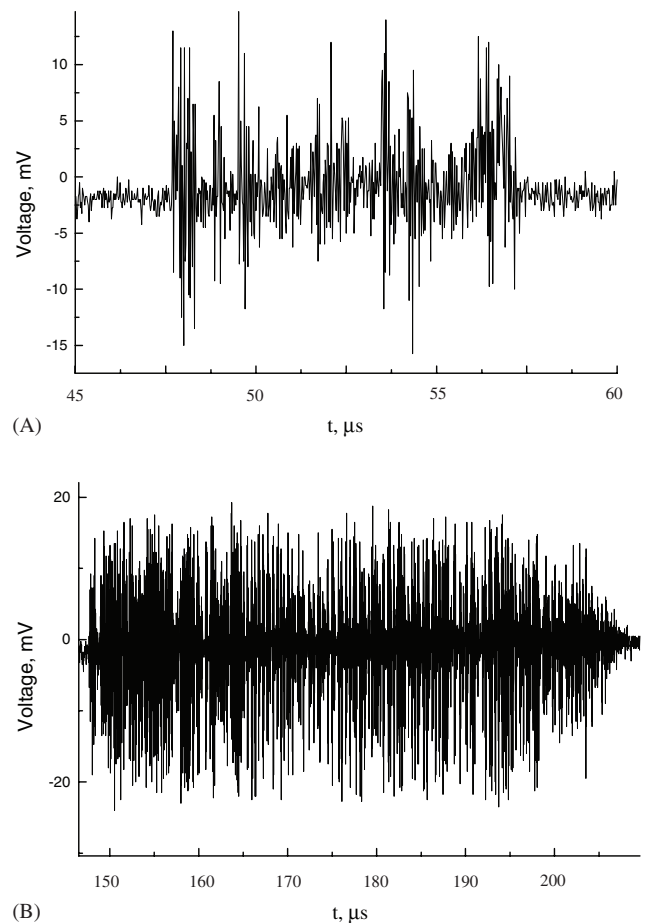


Fig. 4. Two examples of EMR signals observed during drilling of (A) Solenhofen limestone and (B) Ramat Hovav chalk.

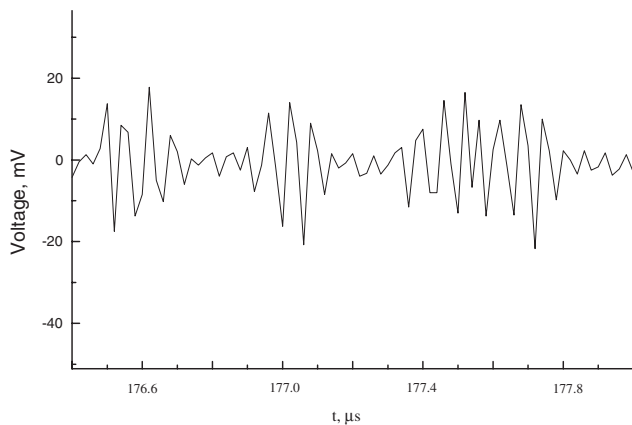


Fig. 5. Three individual EMR signals from chalk drilling.

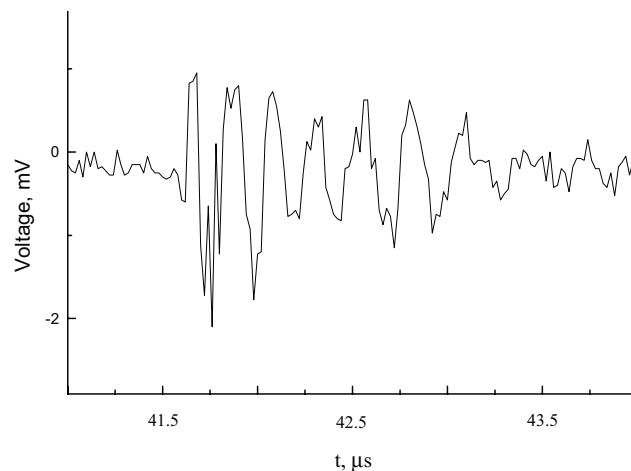


Fig. 7. An individual EMR pulse induced by blasting.

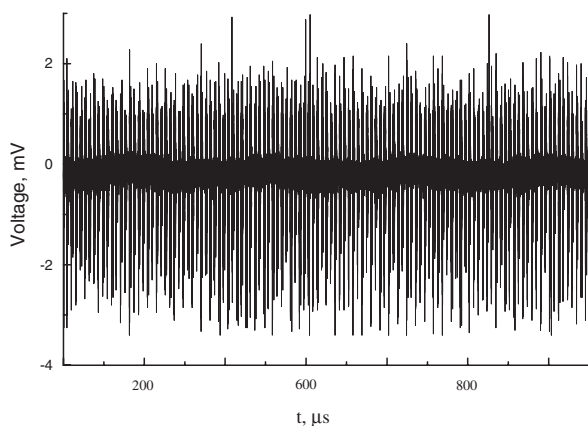


Fig. 6. An EMR string induced by blasting.

EMR pulses excited by drilling is similar to that measured during compression, where however single pulse frequencies never exceeded 10 MHz (Table 1 [9,10]).

3.2. Blasting

Fig. 6 shows $\sim 5\%$ (in time) of the EMR record that was observed during blasting. A detailed analysis of the EMR record shows that the main frequency of the observed pulses lies in the range 2–8 MHz (Table 1), and that the intervals between individual pulses are of about 1–5 μs . The shapes of individual pulses (Fig. 7) that were formed by a digital expansion of Fig. 6 are very similar to those observed during compression and drilling (Figs. 1 and 5). Our analysis shows that it is only the durations of the EMR records that were different. The durations of the EMR records from blasts were similar to those of the explosions themselves $\sim 0.5\text{ s}$ for the more powerful blast (5 t) and $\sim 0.3\text{ s}$ for the second one (1.4 t).

4. Discussion

The experimental results are summarized in Table 1. We now consider the unifying properties and dissimilarities of the different processes. As is known [29], when stress waves propagate through a brittle material, a population of micro-defects are generated and extended. In drilling and blasting the rock is deformed under dynamic conditions, which create high-intensity stress waves. A stress wave of sufficient amplitude (like those created during blasting or drilling) can initiate rock fragmentation at the expense of wave energy [30]. A fragmentation process, such as in drilling or blasting, where numerous cracks are created, is the origin of strings of EMR pulses. A larger stress wave energy leads to a larger fragmentation volume in the rock and, hence to a larger duration of these strings. Therefore, EMR pulse strings, which represent a small volume of rock in drilling are much shorter (2–60 μs , Table 1), than those induced by blasting (~ 0.3 and 0.5 s , Table 1). In comparison, during compression (strain rate 10^{-5} s^{-1}), where these strings stem merely from crack coalescence, the duration of each EMR string never exceeded 30 μs .

Zooming in on the EMR strings induced by blasting shows that both the amplitude and the frequency of individual pulses are different from those obtained in drilling and in compression. Nevertheless an overall comparison of EMR signals, excited by compression, drilling and blasting shows their basic shape to be invariant to the dynamic/quasi-static loading mode. Note that this basic shape was shown previously to be invariant to the fracture mode [10]. The similarity of shape of single EMR pulses, induced by these three processes, therefore enables us to analyze the EMR signals induced by drilling and blasting by the same model we developed earlier for compression [10]. This model allows us to calculate the dimensions of the crack, which was the source of the measured EMR signal. As

we noted above, the time from pulse origin up to its envelope maximum T' is proportional to the crack length, while crack width is inversely proportional to the EMR frequency $f = \omega/2\pi$ [10,12,13]. Hence, the ratio T'/ω is proportional to the crack area S . Our analysis shows that the time from EMR pulse origin up to its envelope maximum T' induced by blasting ranges between 0.01 and 0.5 μs . The ω value of the signals ranges between 16 and $50 \times 10^6 \text{ s}^{-1}$. Hence their ratio T'/ω will be of about $0.06\text{--}1 \times 10^{-14} \text{ s}^2$. The analysis [11] showed that the proportionality coefficient between T'/ω and crack area S was $\sim 3 \times 10^7$. Hence, crack areas induced by blasting include a major fraction whose area is estimated to be of about $0.02\text{--}0.3 \text{ mm}^2$. Note that cracks of similar areas are created at the beginning of compression loading [10].

As noted by Rossmannith et al. [29], the net of fractures induced by blasting can be divided into three zones: a crush zone (near the borehole) of short uniformly distributed radial cracks; an intermediate zone, where short cracks from the crush zone extend; and an outer zone with long radial cracks. Comparison of estimated crack areas (see above) with this model shows that our EMR signals are induced by cracks from the two first zones (crush and intermediate) and can indicate the beginning of a dynamic large-scale failure. These results are similar to those obtained for the origin of quasi-static (compression) and dynamic (drilling) failure in the lab, where EMR pulses were observed along the whole process of failure from the origin of cracking up to rock collapse [10,27].

Acknowledgements

This research No. 244/99-2 was supported by the Israel Science Foundation.

References

- [1] Cress GO, Brady BT, Rowell GA. Sources of electromagnetic radiation from fracture of rock samples in the laboratory. *Geophys Res Lett* 1987;14:331–4.
- [2] Fujinawa Y, Takahashi K. Electromagnetic radiations associated with major earthquakes. *Phys Earth Plan Inter* 1998;105(3–4): 249–59.
- [3] Nitsan V. Electromagnetic emission accompanying fracture of quartz-bearing rocks. *Geoth Res Lett* 1977;4(8):333–6.
- [4] Ogawa T, Oike K, Miura T. Electromagnetic radiation from rocks. *J Geophys Res* 1985;90(d4):6245–9.
- [5] Warwick JW, Stoker C, Meyer TR. Radio emission associated with rock failure: possible application to the great Chilean earthquake of May 22, 1960. *J Geophys Res* 1982;87(b4):2851–9.
- [6] Yamada I, Masuda K, Mizutani H. Electromagnetic and acoustic emission associated with rock fracture. *Phys Earth Plan Inter* 1989;57:157–68.
- [7] Gol'd RM, Markov GP, Mogila PG. Pulsed electromagnetic radiation of minerals and rock subjected to mechanical loading. *Izv Earth Phys* 1975;7:109–11.
- [8] Frid V, Rabinovitch A, Bahat D. Electromagnetic radiation associated with induced triaxial fracture in granite. *Philos Mag Lett* 1999;79:79–86.
- [9] Frid V, Bahat D, Goldbaum J, Rabinovitch A. Experimental and theoretical investigation of electromagnetic radiation induced by rock fracture. *Israel J Earth Sci* 2000;49:9–19.
- [10] Rabinovitch A, Frid V, Bahat D, Goldbaum J. Fracture area calculation from electromagnetic radiation and its use in chalk failure analysis. *Int J Rock Mech Min Sci* 2000;37:1149–54.
- [11] Bahat D, Rabinovitch A, Frid V. Fracture characterization of chalk in uniaxial and triaxial tests by rock mechanics, fractographic and electromagnetic methods. *J Stuct Geology* 2001;23:1531–47.
- [12] Rabinovitch A, Frid V, Bahat D. Parametrization of electromagnetic radiation pulses obtained by triaxial fracture in granite samples. *Philos Mag Lett* 1998;5:289–93.
- [13] Rabinovitch A, Frid V, Bahat D. A note on the amplitude–frequency relation of electromagnetic radiation pulses induced by material failure. *Philos Mag Lett* 1999;79:195–200.
- [14] Rabinovitch A, Bahat D, Frid V. Emission of electromagnetic radiation by rock fracturing. *Z Geol Wiss* 1996;24(3–4):361–8.
- [15] Khatiashvili N. The electromagnetic effect accompanying the fracturing of alkaline halide crystals and rocks. *Izv Earth Phys* 1984;20:656–61.
- [16] Nesbitt AC, Austin B. The emission and propagation of electromagnetic energy from stressed quartzite rock underground. *Tran Inst Electr Eng* 1988;89:53–6.
- [17] Frid V. Rock-burst hazard forecast by electromagnetic radiation excited by rock fracture. *J Rock Mech Rock Eng* 1997;30(4): 229–36.
- [18] Frid V. Electromagnetic radiation method for rock and gas outburst forecast. *J Appl Geophys* 1998;38:97–104.
- [19] Gokhberg M, Gufel'd I, Gershenzon N. Electromagnetic effects due to crustal destruction. *Izv Earth Phys* 1985;21:52–63.
- [20] Rikitake T. Nature of electromagnetic emission precursory to an earthquake. *J Geomagn Geoelectr* 1997;49:1153.
- [21] Gokhberg M, Yoshino T, Morgunov V, Ogawa T. Results of recording of operative electromagnetic precursor in Japan. *Izv Earth Phys* 1982;18:144–6.
- [22] Gokhberg M, Morgunov V, Matveyev V. On the observation of anomalous electromagnetic emission in the epicentral zone of earthquake. *Izv Earth Phys* 1986;22:676–8.
- [23] Gershenzon N, Gokhberg M, Morgunov V. Sources of electromagnetic emissions preceding seismic events. *Izv Earth Phys* 1987;23:96–101.
- [24] Gershenzon N, Gokhberg M, Karakin A. Modelling the connection between earthquake preparation processes and crustal electromagnetic emission. *Phys Earth Plan Inter* 1989;57:129–38.
- [25] Bella F, Bjadji PF, Della Monica J, Zilpimiani DO, Manguladze PV. Observations of natural electromagnetic radiation during earthquakes of central Italy. *Izv Earth Phys* 1992;28:88–94.
- [26] Parrot M, Achache J, Berthelier JJ, Blanc E. High frequency electromagnetic effects. *Phys Earth Plan Inter* 1993;77:65–81.
- [27] Goldbaum J, Frid V, Rabinovitch A, Bahat D. Electromagnetic radiation induced by percussion drilling. *Int J Fract* 2001;23:1531–47.
- [28] Jaeger JC, Cook NGW. *Fundamentals of rock mechanics*. London: Chapman & Hall, 1979.
- [29] Rossmannith HP, Daehnke A, Khasmiller RE, Kouzniak N, et al. Fracture mechanics applications to drilling and blasting. *Fatigue Fract Eng Mater Struct* 1997;20(11):1617–36.
- [30] Gueguen Y, Palciauskas V. *Introduction to the physics of rocks*. Princeton, NJ: Princeton University Press, 1994.